Molecular Cell
Article

Immobilization of Proteins in the Nucleolus by Ribosomal Intergenic Spacer Noncoding RNA

Timothy E. Audas,[1,2] Mathieu D. Jacob,[1,2] and Stephen Lee[1,2,*]
[1]Department of Cellular and Molecular Medicine
[2]Faculty of Medicine
University of Ottawa, Ottawa, ON K1H 8M5, Canada
*Correspondence: slee@uottawa.ca
DOI 10.1016/j.molcel.2011.12.012

SUMMARY

Cellular pathways are established and maintained by stochastic interactions of highly mobile molecules. The nucleolus plays a central role in the regulation of these molecular networks by capturing and immobilizing proteins. Here, we report a function for noncoding RNA (ncRNA) in the regulation of protein dynamics of key cellular factors, including VHL, Hsp70 and MDM2/PML. Stimuli-specific loci of the nucleolar intergenic spacer produce ncRNA capable of capturing and immobilizing proteins that encode a discrete peptidic code referred to as the nucleolar detention sequence (NoDS). Disruption of the NoDS/intergenic RNA interaction enables proteins to evade nucleolar sequestration and retain their dynamic profiles. Mislocalization of intergenic ncRNA triggers protein immobilization outside of the nucleolus, demonstrating that these ncRNA species can operate independently from the nucleolar architecture. We propose a model whereby protein immobilization by ncRNA is a posttranslational regulatory mechanism.

INTRODUCTION

Cellular networks are regulated by the localization of essential factors to the site of action in a timely and efficient manner. While machinery exists in the cytoplasm to facilitate interorganelle molecular targeting, no known intracompartmental trafficking pathways have been established. Therefore, it is believed that proteins rely on an energy-independent stop-and-go mechanism, whereby highly mobile molecules diffuse throughout an organelle's cellular milieu randomly scanning for appropriate and stable associations (reviewed in Hager et al., 2009; Misteli, 2001b). Compartmentalization in cytoplasmic domains such as stress granules or within the numerous subnuclear bodies presents a unique challenge for molecular dynamics because these regions are not membrane bound and, therefore, are unable to confine their resident molecules. Intuitively, one might assume these domains form through highly stable interactions of molecules at specific sites. However, it has been well established that resident molecules retain their mobility and are in a constant state of flux in and out of these regions (Andersen et al., 2005; Chen and Huang, 2001; Dundr et al., 2002; Houtsmuller et al., 1999; Kedersha et al., 2000; Kruhlak et al., 2000; Matera et al., 2009; Phair and Misteli, 2000). Therefore, formation of these structures likely relies on a model of stochastic self-organization around essential structural components (Kaiser et al., 2008), where stable interactions enhance the steady-state residency time of targeted molecules (Misteli, 2001a).

The prototypical subnuclear domain is the nucleolus, the site of rRNA synthesis, processing and ribosomal assembly (Tschochner and Hurt, 2003). These bodies form around a scaffolding of ribosomal DNA (rDNA) tandem repeats. Each repeat consists of an rDNA enhancer/promoter that is located directly upstream of its ribosomal RNA (rRNA) coding sequence and separated by a large intergenic spacer (IGS) region made up of highly repetitive DNA (McStay and Grummt, 2008) that is classically perceived to be transcriptionally inactive (Hillis and Dixon, 1991). Although numerous proteins are known to reside in the nucleolus to facilitate rRNA synthesis, mapping of the nucleolar proteome has identified many proteins that possess functions not generally ascribed to ribosomal biogenesis (Andersen et al., 2002, 2005; Scherl et al., 2002; Shou et al., 1999), suggesting that the nucleolus may be plurifunctional. One emerging field of nucleolar study involves subnuclear reorganization in response to environmental stimuli (reviewed in Boulon et al., 2010). Hsp70 was one of the first molecules to demonstrate a shift in localization from predominantly diffuse cytoplasmic to nucleolar upon incubation at 42°C (Welch and Feramisco, 1984). Since this initial observation, numerous other stresses have been shown to target proteins to the nucleolus, including acidosis (Mekhail et al., 2004), ribosomal stress (Lohrum et al., 2003; Weber et al., 1999), serum starvation, and DNA damage (Stark and Dunlop, 2005). Photobleaching analysis of VHL and MDM2 has revealed that, under standard growth conditions, these molecules are highly mobile (Mekhail et al., 2005) extranucleolar ubiquitin ligases that are capable of efficiently degrading their substrates (Honda et al., 1997; Maxwell et al., 1999). However, in stark contrast to the highly dynamic nature of resident nucleolar proteins (Andersen et al., 2005; Chen and Huang, 2001; Dundr et al., 2002), targeting of VHL and MDM2 to the nucleolus in response to acidosis and ribosomal stress, respectively, renders these proteins immobile (Mekhail et al., 2005) and inhibits their ubiquitin ligase activity. Therefore, the nucleolar proteome appears to be subdivided into two

classifications: 1) dynamic resident proteins, which carry out an active cellular function, such as ribosomal biogenesis, and 2) immobile detained proteins, which are retained under certain cellular conditions within the nucleoli away from their downstream effectors (Mekhail et al., 2005), a process that renders them functionally inert (Misteli, 2001b).

Unlike the well-characterized amino acid sequences required for trafficking proteins to most cellular organelles, nucleolar targeting appears to be mediated by the association of proteins with components of the nucleolar architecture (Jacobson et al., 1995; Shaw and Jordan, 1995). To date, several putative nucleolar localization signals have been identified, which consist of highly charged arginine or lysine residues (reviewed in Emmott and Hiscox, 2009). Given the conflicting dynamic properties of resident and detained nucleolar proteins, it seems highly likely that these two classifications would possess divergent nucleolar targeting elements. The identification of inducibly detained nucleolar proteins in response to multiple environmental cues, most notably relocalization of VHL during acidosis (Mekhail et al., 2004), translocation of MDM2 under ribosomal stress (Lohrum et al., 2003; Rubbi and Milner, 2003; Weber et al., 1999), and heat shock-mediated sequestration of Hsp70, begs the question of whether these conditions share a common mechanism of static nucleolar detention.

In this report, we identify *cis*- and *trans*- regulatory elements that are essential and sufficient for the immobilization of proteins within the nucleolus. We demonstrate the presence of a group of inducible noncoding nucleolar RNA (ncRNA) molecules derived from stimuli-specific loci within the IGS of the rDNA. These ncRNA regulate molecular networks by capturing and immobilizing specific proteins that harbor a discrete code, referred to as the nucleolar detention sequence (NoDS), in response to environmental cues.

RESULTS

Immobilization of Protein by Intergenic Spacer ncRNA

Protein targeting to the nucleolus upon acidification of the extracellular milieu is mediated by the NoDS motif (Mekhail et al., 2005, 2007). To better understand the shift in localization and mobility of NoDS-containing proteins, such as VHL, DNA (cytosine-5)-methyltransferase 1 (DNMT1), and the delta catalytic subunit of DNA polymerase (POLD1) (Figure 1A), we wanted to determine which region of the nucleolar architecture was responsible for the detention of proteins during acidosis. To do so, chromatin immunoprecipitation (ChIP) was performed, scanning the entire rDNA cassette (Figure 1B) for protein binding sites. Under neutral conditions, none of the proteins tested associated with the rDNA (Figure 1C). Conversely, acidified cells had VHL-GFP as well as endogenous POLD1 specifically bound to a discrete region of the IGS that was located 28 kb downstream of the rRNA transcriptional start site (Figure 1C). Partial proteolysis of sonicated lysates with trypsin revealed that VHL-GFP isolated from acidotic cells was more sensitive to enzymatic digestion compared to neutral lysates, whereas RNase but not DNase pretreatment triggered a reversion toward the neutral conformation (Figure S1A available online). Based on these observations, we reasoned that an RNA species might be involved in the capture of NoDS-containing proteins by the 28 kb locus of the IGS. RT-PCR using a primer set spanning IGS 27.3–28.0 kb revealed the presence of a temporarily induced transcript in multiple independent cell lines during acidosis treatment (Figures 1D and S1B). Northern blot utilizing a probe from the same region detected an ~325 nucleotide RNA that was induced and remained elevated during the course of acidosis treatment (Figures 1D and S1C). Scanning by RT-PCR with multiple overlapping primers showed that although the entire IGS_{28} locus is expressed, a more abundant transcript is present between 27.35–27.77 kb (Figure S1D), consistent with the RNA species detected by northern blotting. These data suggest that the transcription product detected by RT-PCR and emanating from the IGS undergoes a processing event to produce the smaller form, which remains elevated during the stimulus and is observed by northern blot (Figure 1D). Sequence analysis confirmed that this acidosis-induced RNA, hereafter referred to as IGS_{28}RNA, originates from the 28 kb region of the rDNA cassette (Figure S1E). At low pH (Figure S1F), RNA polymerase I (Figure S1G) synthesizes IGS_{28}RNA at moderate levels (Figure S1H) from the same strand as the rRNA (Figures 1E and S1I). This nonpolyadenylated transcript (Figure S1J) accumulates within the nucleolar compartment (Figures 1F, S1K, and S1L), suggesting that it is an ncRNA because it is not available for translation by cytoplasmic polysomes. RNA immunoprecipitation of acidified cells further indicated an association of VHL with IGS_{28}RNA but not with the GAPDH or β-actin transcripts (Figure 1G). Together these data identify a pH-regulated ncRNA that is produced from the heart of the nucleolar IGS.

To test the role of IGS_{28}RNA in nucleolar sequestration, we produced cell lines stably expressing independent shRNAs targeted against different regions of IGS_{28}RNA (shRNA-28; Figure S1E), which were capable of efficiently reducing the transcript levels (Figure 2A). Under neutral pH conditions, none of the shRNAs altered the localization of VHL-GFP or endogenous POLD1 (Figures 2B, 2C, S2A, and S2B). However, shRNA-28 inhibited pH-dependent nucleolar localization of VHL-GFP in MCF-7 (Figure 2B and Figure S2A) and HEK293 (Figure S2C) cells and endogenous POLD1 (Figures 2C and S2B), whereas the control shRNA had no effect. Photobleaching analysis showed that VHL-GFP and DNMT1-GFP remained highly mobile in cell lines expressing shRNA-28, even during acidosis (Figures 2D, 2E, 2F, and 2G). This effect was reproducible for several additional NoDS-containing proteins that were immobilized by the nucleolus during acidosis but retained their dynamic profiles in shRNA-28-expressing cells (Figures S2D and S2E).

We next engineered a plasmid that expressed IGS_{28}RNA ($pcIGS_{28}$) to test whether this ncRNA can immobilize proteins outside of the nucleolar architecture. RT-PCR assays revealed that $pcIGS_{28}$ expressed transcripts accumulated in the nuclear and cytosolic fractions of the cell under neutral pH conditions (Figure 3A). Interestingly, VHL-GFP displayed a distinct cytoplasmic punctate pattern in cells containing $pcIGS_{28}$ (Figure 3B), whereas the localization of other unrelated proteins, such as p27 and Hsp110, were unaffected (Figure S3A). Cells transfected with a promoterless construct of IGS_{28}RNA ($pGEM\text{-}IGS_{28}$) were unable to trigger cytoplasmic protein aggregation, indicating that the DNA sequence alone cannot mediate

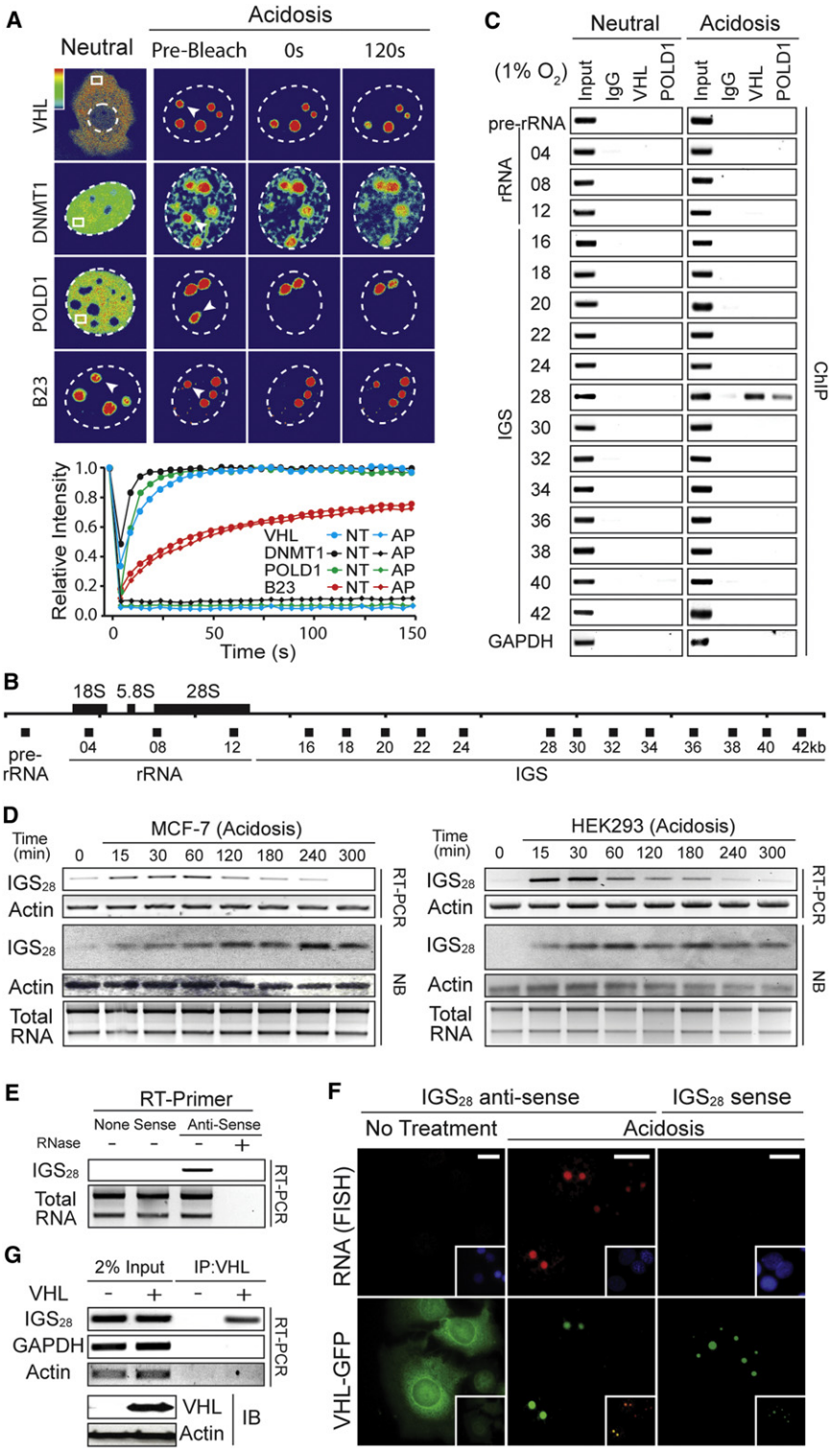

Figure 1. A Discrete Locus of the IGS Produces a pH-Inducible ncRNA

(A) Acidosis triggers nucleolar immobilization of proteins. MCF-7 cells transfected with VHL-GFP, DNMT1-GFP, POLD1-GFP and B23-GFP were left untreated (NT) or grown for 20 hr at 1% oxygen in acidosis permissive (AP) media prior to FRAP analysis. Cells were bleached in the indicated region (squares) or nucleoli (arrowhead) and allowed to recover. Times postbleaching are indicated on pseudocolored images with high (red) to low (blue) intensity, indicating changes in fluorescence (upper panel). Fluorescence recovery kinetics of the bleached regions were quantified and presented below as the mean relative intensity of at least 10 datasets (lower panel).

(B) The 43 kb human rDNA cassette with the primer pairs used for ChIP and RT-PCR analysis.

(C) Acidosis-mediated sequestration occurs at the IGS_{28} locus. MCF-7 cells grown at 1% oxygen in neutral and acidosis-permissive media underwent ChIP analysis for adenovirus-expressed VHL-GFP and endogenous POLD1 binding sites.

(D) Extracellular acidification induces IGS_{28}RNA. Cultured MCF-7 (left) and HEK293 (right) cells were grown in pH6.0 media for the indicated times and induction of the IGS_{28}RNA was analyzed by semiquantitative RT-PCR and northern blotting (NB). β-actin and total RNA were included as controls.

(E) IGS_{28}RNA is expressed from the same strand as rRNA. Semiquantitative RT-PCR using no primer or IGS_{28}-specific sense (same strand as the rRNA) or antisense primers. RNA was extracted from acidotic cells and left untreated or RNase digested.

(F) IGS_{28}RNA is localized to the nucleolus. VHL-GFP transfected MCF-7 cells were acidified and IGS_{28}RNA was detected by fluorescent in situ hybridization using digoxigenin-labeled sense and anti-sense probes (red). Hoechst (blue) and merged (yellow) images are inset. Bars, 10 μm.

(G) IGS_{28}RNA immunoprecipitates with VHL. Acidified MCF-7 cells with (+) or without (–) VHL-GFP were precipitated and screened for the presence of IGS_{28}RNA, GAPDH and β-actin transcripts. VHL and β-actin protein was detected by immunoblotting.

aggregation (Figure 3B). Photobleaching analysis showed that transfection with pcIGS$_{28}$, but not the control plasmids, immobilized VHL-GFP in the cytoplasm (Figures 3C, S3B, and Movie S1). This was not due to unforeseen toxicity because pcIGS$_{28}$-expressing cells remained viable during and after photobleaching (Figure S3C and Movie S1). Additionally, the cytoplasmic stress granule resident protein Tia-1 (Anderson and Kedersha, 2009; Buchan and Parker, 2009) did not significantly colocalize with VHL-GFP in pcIGS$_{28}$-expressing cells under normal growth conditions or upon stress granule induction with sodium arsenite (Figure S3D). Photobleaching analysis demonstrated that both cytoplasmic (PABP1) and nuclear (HSF1) stress granule resident proteins remained highly mobile (Figure 3C,

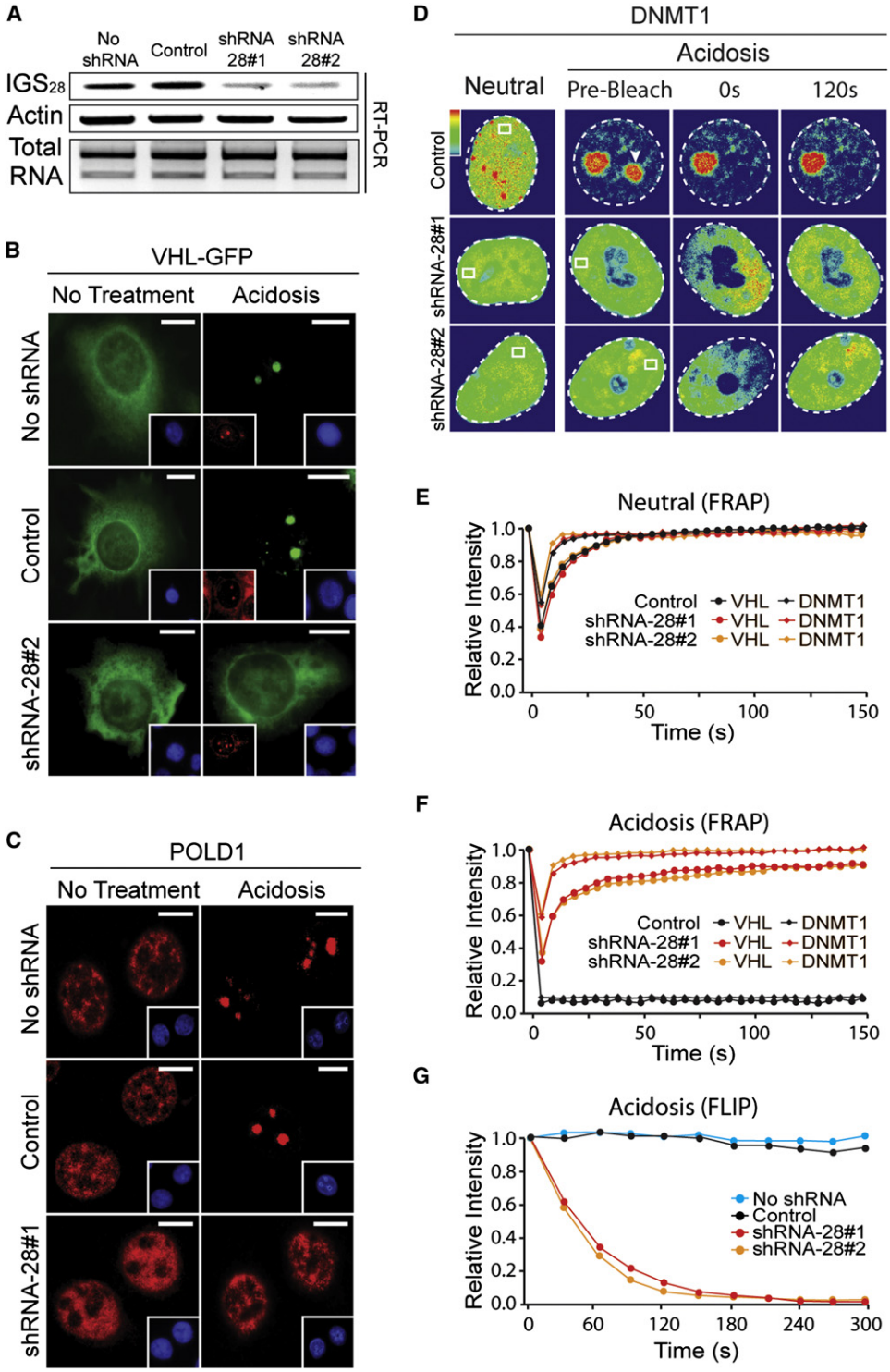

Figure 2. IGS_{28}RNA Is Required for Nucleolar Detention during Acidosis

(A) Stable expression of shRNA inhibits IGS_{28}RNA. MCF-7 cell expressing shRNA targeted to a scrambled sequence (control) or two different sites on IGS_{28}RNA (shRNA-28#1 and shRNA-28#2) were exposed to acidosis prior to semiquantitative RT-PCR.

(B) Knockdown of IGS_{28}RNA inhibits the sequestration of VHL-GFP. Cell lines expressing shRNA were infected with an adenovirus-expressing VHL-GFP and allowed to acidify under hypoxic conditions. The nucleolar protein B23 (inset red) and Hoechst-stained DNA (inset blue) was detected.

(C) Acidosis-mediated nucleolar sequestration of endogenous POLD1 is inhibited by IGS_{28}RNA knockdown. Immunostaining of endogenous POLD1 (Hoechst inset) in shRNA knockdown cells left untreated or allowed to acidify.

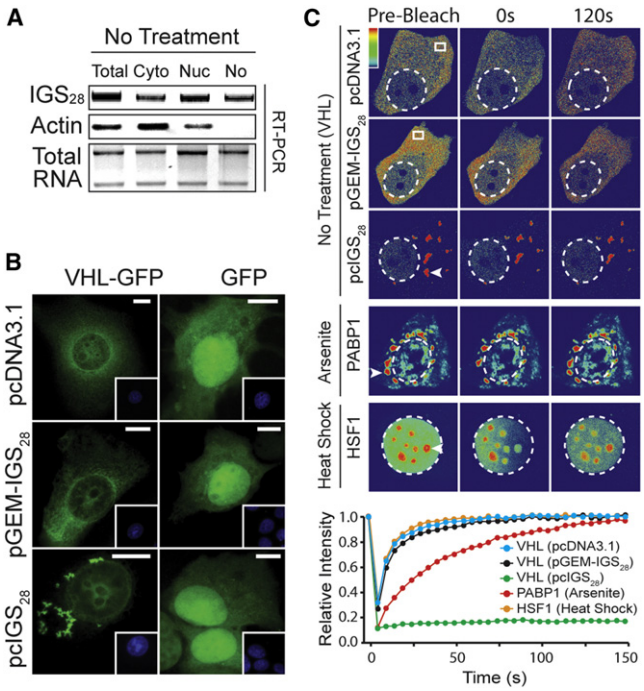

Figure 3. Misexpression of IGS_{28}RNA Immobilizes Proteins Outside of the Nucleolus

(A) Exogenously-expressed IGS_{28}RNA ($pcIGS_{28}$) is present throughout the cell. Untreated MCF-7 cells were fractionated into total, cytoplasmic (Cyto), nuclear (Nuc) and nucleolar (No) RNA, prior to RT-PCR for IGS_{28}RNA and β-actin.

(B) IGS_{28}RNA triggers cytoplasmic aggregation. MCF-7 cells expressing VHL-GFP or GFP alone were transfected with pcDNA3.1, pGEM-IGS_{28} or $pcIGS_{28}$. DNA staining with Hoectsh is inset.

(C) Components of IGS_{28}RNA aggregates are immobile, while stress granule components remain dynamic. FRAP analysis of untreated MCF-7 cells expressing VHL-GFP and the effector plasmids pcDNA3.1, pGEM-IGS_{28} or $pcIGS_{28}$, arsenite treated cells expressing the cytoplasmic stress granule marker protein GFP-PABP1 and the nuclear stress granule marker HSF1-GFP in cells heat shocked for 10 min. Bleaching of the cytoplasmic region (square) or aggregate (arrowhead) was performed and the corresponding kinetics of recovery is included in the lower panel. Bars, 10 μm.

Movie S2, and Jolly et al., 1999; Kedersha et al., 2000), further distinguishing these structures from those produced by endogenous IGS_{28}RNA and $pcIGS_{28}$. Put together, data from Figures 1, 2, and 3 identified a class of acidosis-induced ncRNA originating from the IGS involved in the capture and immobilization of proteins by the nucleolar architecture.

Stimuli-Specific Loci of the IGS Produce Distinct ncRNAs Involved in the Immobilization of Proteins

Heat shock is a well-known physiological stimulus that triggers nucleolar sequestration of Hsp70 as well as many other proteins. Because the mechanism of heat shock-dependent nucleolar sequestration remains unknown, we reasoned that it might follow a process similar to acidosis-mediated detention involving IGS_{28}RNA. Unexpectedly, we observed that endogenous Hsp70 was captured by positions 16 and 22 kb of the IGS, rather than the acidosis-specific position 28 kb (Figure 4A). Likewise, transcriptional stress caused binding of MDM2-GFP prominently at position 20 kb, and also at other IGS regions (Figure 4A), in a PML-dependent manner (Figures S4A and S4B and Bernardi et al., 2004). Photobleaching analysis confirmed that proteins sequestered in the nucleolus during heat shock and transcriptional stress, such as Hsp70, RNF8, MDM2, and APC2, were immobile (Figure 4B). Here, we used a variant of Hsp70 (Hsp70v-GFP) that precisely parallels the kinetics and completeness of endogenous Hsp70 nucleolar sequestration because the exogenous full-length protein is only partially captured by the nucleolus, rendering photobleaching impractical (Figure S4C and Milarski and Morimoto, 1989). These data suggest that the IGS is organized into multiple stimuli-specific loci that are involved in the immobilization of proteins.

Given the upregulation of IGS_{28}RNA during acidosis, we hypothesized that a similar RNA expression profile would be observed from heat shock protein binding sites 16 and 22 kb. RT-PCR demonstrated the presence of heat shock-inducible ncRNAs (Figures 5A and S5A) expressed from these loci at moderate levels (Figure S5B) from the same strand as the rRNA (Figure S5C) during Hsp70 sequestration (Figure S5D), now designated IGS_{16}RNA and IGS_{22}RNA. PCR analysis of the IGS 21 to 22 kb region from genomic DNA and total RNA produced amplicons of different sizes (Figure 5B). Sequence analysis of multiple cDNAs identified an ~300 bp transcript containing an internal processing event (Figure S5E); similarly sized heat shock-inducible transcripts were also observed by northern blotting using a probe from this region (Figures 5A and S5C). A cell line expressing shRNA, which efficiently ablates IGS_{22}RNA (shRNA-22) (Figure 5C), reduced the binding of endogenous Hsp70 at the 22 kb locus (Figure 5D) and considerably delayed its nucleolar localization during heat shock treatment (Figure 5E). Expression of IGS_{16}RNA remained unfettered (Figure 5C) in the shRNA-22 cell line, thereby allowing these cells to recruit Hsp70, albeit with slower kinetics. Purified GST-Hsp70 directly bound in vitro transcribed IGS_{22}RNA but not a control neomycin resistance (Neo^R) transcript. Interestingly, GST-Hsp70 also failed to associate with the in vitro transcribed IGS 21–22 kb genomic sequence (IGS_{22}[g]) (Figure 5F). Overexpression of IGS_{22}RNA ($pcIGS_{22}$) triggered nuclear/cytoplasmic aggregation of endogenous Hsp70 (Figure 5G) and immobilization of Hsp70v-GFP (Figure 5H) in a manner reminiscent of the effect of $pcIGS_{28}$ on VHL-GFP (Figures 3B and 3C). In contrast, overexpression of IGS_{22}(g) ($pcIGS_{22}$[g]) had no effect on endogenous Hsp70 or Hsp70v-GFP, further emphasizing the importance of the processing event in producing functional IGS_{22}RNA

(D) The mobility of DNMT1-GFP under neutral and acidotic conditions in shRNA knockdown cell lines. Cells transfected with DNMT1-GFP were left untreated or exposed to acidosis prior to photobleaching of targeted regions (square) within the nucleus (dashed circles) or specific nucleoli (arrowhead), followed by recovery for the indicated times.

(E and F) Quantification of recovery after bleaching of VHL-GFP and DNMT1-GFP in MCF-7 cells expressing shRNA under neutral (E) or acidotic (F) conditions.

(G) Quantification of fluorescence loss in photobleaching (FLIP) of VHL-GFP in acidotic MCF-7 and shRNA containing cells. Bars, 10 μm.

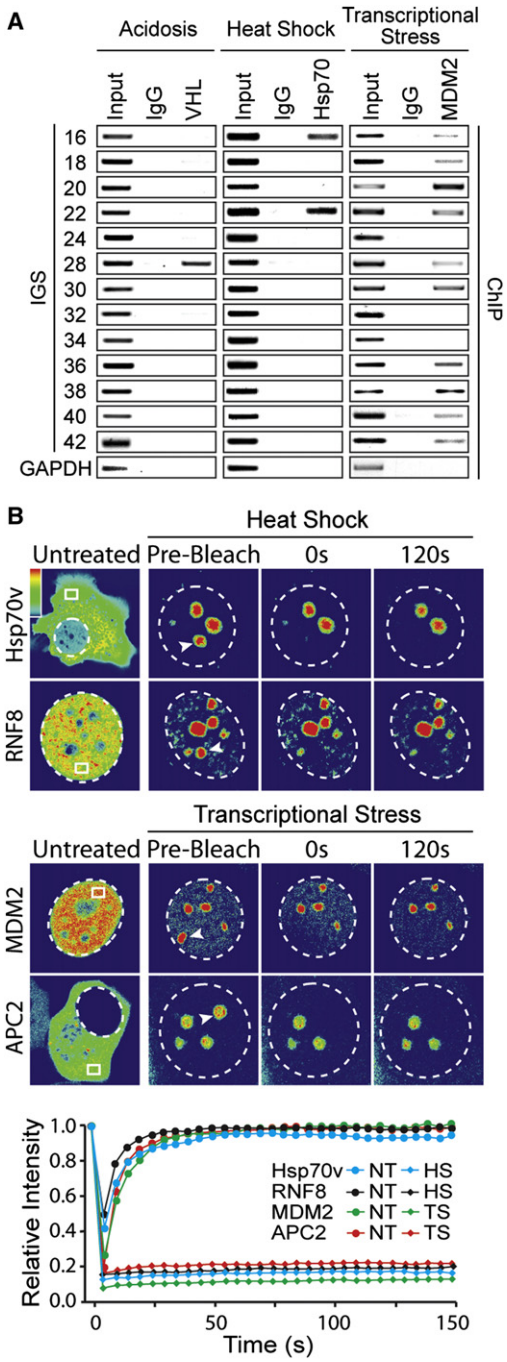

Figure 4. Environmental Cues Trigger Nucleolar Immobilization of Proteins at Different Loci of the IGS

(A) Acidosis, heat shock, and transcriptional stress capture proteins at different loci. ChIP mapping of VHL-GFP, endogenous Hsp70 and MDM2-GFP in MCF-7 cells left untreated or exposed to acidosis, heat shock or transcriptional stress.

(B) Proteins are statically detained in the nucleolus during heat shock (HS) and transcriptional stress (TS) treatment. Photobleaching images of cells expressing Hsp70v-GFP and RNF8-GFP during heat shock treatment (upper panel) or MDM2-GFP and APC2-GFP under transcriptional stress (middle panel). Bleached regions were indicated and quantification of recovery kinetics is included as the mean of 10 datasets (lower panel).

(Figures 5G and 5H). Analysis of the entire IGS by high cycle number RT-PCR revealed multiple ncRNAs expressed from across the IGS, including the sites of transcriptional stress capture (Figure S4D). Because numerous sites appear responsible for stress-mediated nucleolar detention of MDM2 and APC2 (Figure 4B) we used high levels of a general transcriptional inhibitor prior to stress treatment to prevent IGSRNA expression. Pretreatment of cells inhibited nucleolar detention of MDM2-GFP during transcriptional stress (Figures S4E and S4F), further supporting a role for IGS ncRNA in protein immobilization.

We next asked whether the stimuli-specific IGS loci operate independently. RT-PCR analysis demonstrated that IGS_{28}RNA is induced by acidosis and unresponsive to heat shock treatment, while IGS_{16}RNA/IGS_{22}RNA accumulated only at 42°C but not at low pH (Figure 6A). Furthermore, disruption of one locus does not affect the function of the others because inhibition of the acidosis-induced IGS_{28}RNA does not prevent nucleolar sequestration of Hsp70 during heat shock treatment (Figure 6B). Likewise, silencing IGS_{22}RNA (Figure 6A) had no effect on pH-dependent nucleolar sequestration of Hsp70 (Figure 6B), which is also captured by the nucleolus at low pH (Mekhail et al., 2007). ChIP analysis further confirmed that the stimuli-specific loci are functionally autonomous because Hsp70 is captured by the 28 kb region during acidosis and the 16/22 kb regions upon heat shock treatment (Figure 6C). Consistent with the ChIP data, Hsp70 was capable of associating in vitro and in vivo with the IGS_{28}RNA (Figures 6D, 6E, and S6A), and silencing of this transcript was sufficient to abrogate pH-dependent capture of Hsp70 by nucleoli (Figures 6B and S6B). Put together, these results demonstrate that the IGS is a complex transcriptional unit composed of multiple stimuli-specific loci that operate independently to immobilize proteins as a function of environmental cues.

The NoDS Is a Common Peptidic Code That Interacts with IGS ncRNA to Mediate Immobilization of Proteins

As mentioned above, pH-dependent nucleolar sequestration is mediated by a discrete, position-independent code, referred to as the NoDS (Mekhail et al., 2007), which is defined by the mandatory presence of two arginine residues followed by a leucine or isoleucine ($RR^{L}/_{I}$) and at least two hydrophobic $Lh^{L}/_{V}$ triplets (where h represents any hydrophobic residues) scattered throughout the length of the protein. Deletion of the arginine motifs of VHL (VHLΔRM-GFP) prevents nucleolar detention during acidosis and immobilization in cytoplasmic aggregates upon ectopic IGS_{28}RNA expression (Figures 7A and S7A). Removal of the arginine motif of Hsp70 prevented heat shock-mediated nucleolar localization of full-length Hsp70-GFP (Figure S4C), as well as nucleolar detention and $pcIGS_{22}$-induced cytoplasmic immobilization of Hsp70v-GFP (Figures 7B and 7C). Additionally, disruption of the $RR^{L}/_{I}$ domains of RNF8-GFP inhibited its nucleolar sequestration during heat shock (Figure S7B).

To highlight its sufficiency, we created a minimal NoDS containing one arginine motif and two hydrophobic repeats. Numerous combinations were possible because many proteins contain multiple copies of these domains. Interestingly, one of the molecules we engineered (RRIHSYRLLVNQTELFV), referred

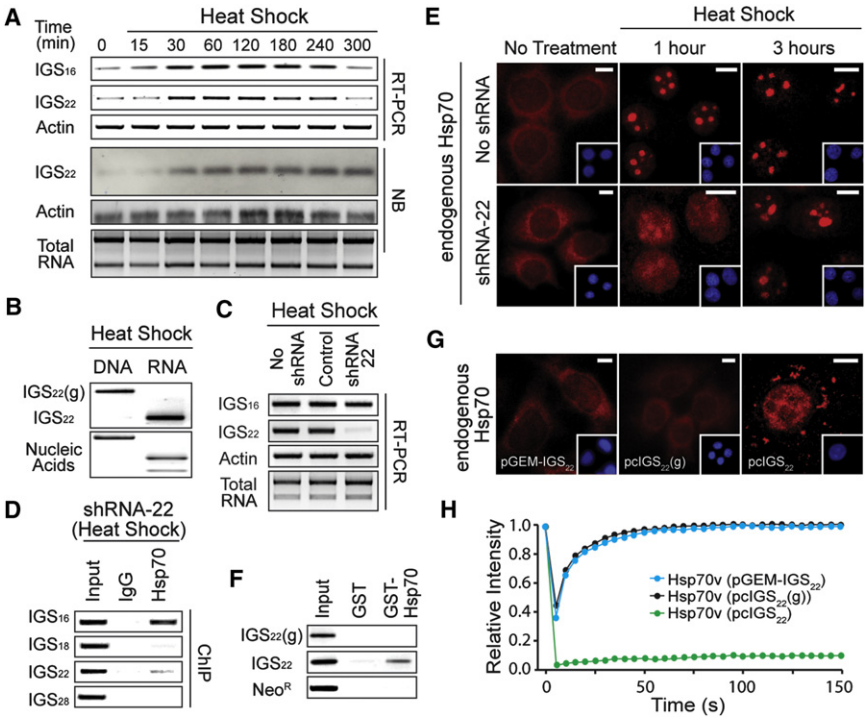

Figure 5. Hsp70 Nucleolar Sequestration Is Regulated by IGSRNA

(A) Induction of IGS_{16}RNA and IGS_{22}RNA during heat shock. MCF-7 cells were transferred from normal growth conditions to 42°C for the indicated times prior semiquantitative PCR and Northern blotting (NB) of IGS_{16}RNA and IGS_{22}RNA. Total RNA and β-actin were included as a loading control.

(B) IGS_{22}RNA undergoes RNA processing. Genomic DNA and total RNA were isolated from heat shock treated cells and amplified with the same primers against the IGS_{22} region, producing the genomic (IGS_{22}[g]) and RNA (IGS_{22}) amplicons.

(C) Stable knockdown of IGS_{22}RNA in MCF-7 cells. Parental MCF-7 (no shRNA), control shRNA (control) and IGS_{22}RNA (shRNA-22) knockdown cells were heat shocked for 1 hr prior RT-PCR of the IGS transcripts.

(D) Hsp70 binding to the IGS_{22} locus during heat shock is inhibited in IGS_{22}RNA knockdown cells. ChIP analysis of endogenous Hsp70 during a 3 hr heat shock treatment in shRNA-22 expressing cells.

(E) Hsp70 nucleolar detention is delayed in IGS_{22}RNA knockdown cells. Parental MCF-7 and IGS_{22}RNA ablated cells were left untreated or heat shocked for 1 and 3 hr as indicated prior to immunostaining for endogenous Hsp70, with Hoechst DNA staining inset.

(F) Hsp70 precipitates with IGS_{22}RNA in vitro. GST and GST-Hsp70 were used to precipitate in vitro synthesized Neo^R mRNA or IGS_{22}RNA transcribed from a template containing the IGS_{22} genomic (IGS_{22}[g]) or IGS_{22}RNA (IGS_{22}) derived sequences. Precipitation was detected by semiquantitative RT-PCR, with a 10% input control.

(G) Processing of IGS_{22}RNA mediates Hsp70 aggregation. Cells transfected with pGEM-IGS_{22}, pcIGS$_{22}$(g) and pcIGS$_{22}$ were immunostained for Hsp70 with Hoechst inset.

(H) Quantification of FRAP experiments in MCF-7 cells transfected with Hsp70v-GFP and the effector plasmids pGEM-IGS_{22}(g), pcIGS$_{22}$(g) and pcIGS$_{22}$. Bars, 10 μm.

to as a reconstituted NoDS (recNoDS), was detained by the nucleolus under all conditions tested and was immobilized in the cytoplasm by pcIGS$_{22}$ and pcIGS$_{28}$ (Figures 7D and 7E). Furthermore, in vitro experiments using synthesized rhodamine-labeled recNoDS molecules showed that the peptides remained soluble in the buffer solution; however, precipitation could be triggered through supplementation with in vitro transcribed IGS_{28}RNA or IGS_{22}RNA but not the unrelated Neo^R mRNA transcript (Figure 7F). In contrast, a peptide in which the arginine residues were substituted with alanines or an irrelevant peptide encompassing amino acids 21–37 of VHL, failed to precipitate even in the presence of the IGS transcripts. Together, these results suggest the generic NoDS is the peptidic motif capable of mediating a protein's interaction with IGS ncRNA to facilitate nucleolar immobilization.

DISCUSSION

In this report, we provide general insight into posttranslational regulation of protein function through ncRNA-mediated modulation of protein dynamics. The data shown here demonstrate that the intergenic spacer of the rDNA cassette is a complex transcriptional unit that is organized into different loci, from which RNA expression is induced in response to specific environmental cues. The ncRNAs associate with a discrete peptidic code, the NoDS, to target proteins for immobilization by the nucleolar architecture. Silencing of condition-specific IGSRNA prevents immobilization of NoDS-containing proteins and their complexes by the nucleolus. The independence of these loci is striking because repression of the heat shock loci does not inhibit acidosis-mediated immobilization and vice versa. Furthermore, ectopic mislocalization of IGSRNAs results in protein aggregation and detention in other regions of the cell, emphasizing the ability of these ncRNAs to regulate protein dynamics. Together, these data demonstrate the existence of a class of ncRNA involved in stimuli-specific nucleolar immobilization of proteins.

Assembly of cellular structures and molecular networks relies on the intrinsic dynamic properties of molecules. This raises the important question as to whether the dynamic nature of these components could be a site of regulation. The observation that reduced protein mobility is generally linked to inactivation (Misteli, 2001b; Phair and Misteli, 2000) would suggest this is the case. Here, we demonstrate a stimuli-mediated mechanism for modulating protein dynamics by ncRNA. Although these IGS ncRNAs appear to target proteins to a subnuclear domain in a similar manner to other nucleating transcripts, such as $MEN^{\epsilon/\beta}$ (Clemson et al., 2009; Mao et al., 2011; Sasaki et al., 2009), satellite III (Jolly et al., 1999, 2004; Rizzi et al., 2004), and heat shock RNA omega (Lakhotia, 1989), they differ fundamentally in their ability to modulate target protein mobility. Furthermore, the

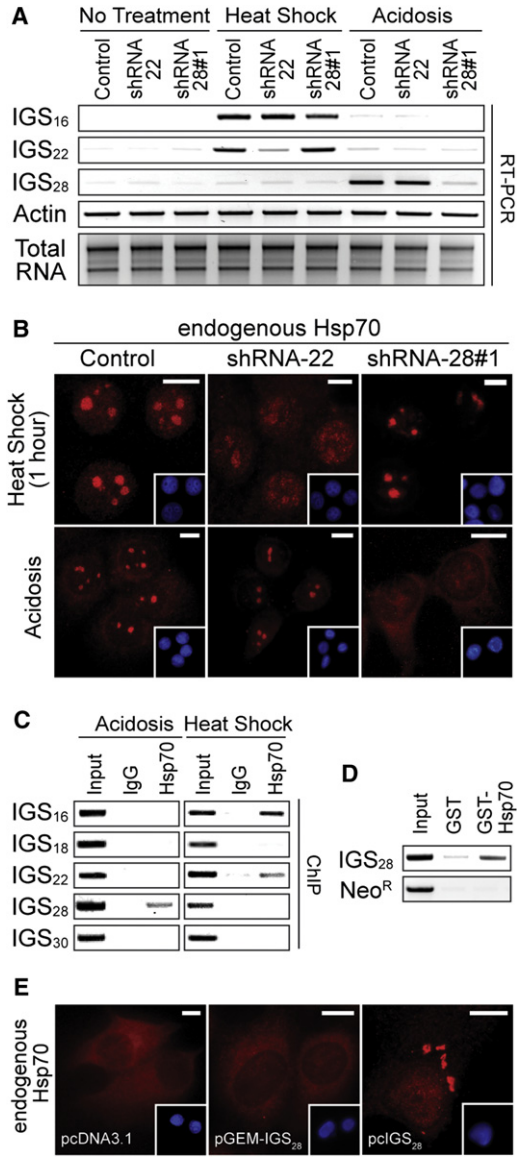

Figure 6. IGSRNA Loci Function Independently

(A) Independent induction of stimuli-specific IGSRNA loci. MCF-7 cells stably expressing shRNA targeting a scrambled sequence (control), IGS_{22}RNA (shRNA-22) or IGS_{28}RNA (shRNA-28#1) were left untreated or exposed to heat shock or acidosis for 1 hr prior to semiquantitative RT-PCR for IGS_{16}RNA, IGS_{22}RNA, IGS_{28}RNA and β-actin.

(B) Disruption of stimuli-specific loci does not inhibit sequestration under another environmental cue. Endogenous Hsp70 was detected in control, shRNA-22 and shRNA28#1 MCF-7 cells exposed to 42°C (1 hr) or acidosis (3 hr). Hoechst is inset in blue.

(C) Nucleolar detention at IGS loci is condition specific. ChIP analysis of MCF-7 cells for endogenous Hsp70 during acidosis and heat shock.

(D) Hsp70 can precipitate IGS_{28}RNA in vitro. In vitro synthesized IGS_{28}RNA (IGS_{28}) or Neo^R mRNA were combined with GST and GST-Hsp70 and allowed to precipitate, prior to detection by semiquantitative RT-PCR.

(E) In vivo Hsp70 aggregation can be triggered by IGS_{28}RNA overexpression. MCF-7 cells transfected with $pcIGS_{28}$ or the control plasmids pcDNA3.1 or $pGEM\text{-}IGS_{28}$ were immunostained for endogenous Hsp70 and counterstained with Hoechst (inset). Bars, 10 μm.

targeted proteome of these other nucleating transcripts is generally limited to components of the transcription machinery (Fox and Lamond, 2010; Jolly and Lakhotia, 2006), whereas IGSRNA is capable of recruiting/immobilizing a diverse array of molecules, including DNMT1, Hsp70, POLD1, and VHL. Recognition of these transcripts appears to occur via the NoDS, a domain that is present in numerous human proteins. These NoDS motifs differ from the classical arginine-rich nucleolar localization signals because they require the presence of multiple hydrophobic repeats and substitution of arginine residues with lysine renders them functionally inert (Emmott and Hiscox, 2009; Mekhail et al., 2007). NoDS-containing proteins often contain several highly variable arginine and hydrophobic motifs, suggesting that these domains may trigger nucleolar detention in response to multiple environmental cues. Additionally, proteins can be immobilized by simply associating with NoDS-containing proteins, providing another level of regulatory complexity to the system. For example, MDM2 and Cullin-2 are sequestered to the nucleolus by assembling with the NoDS-containing proteins PML and VHL, respectively (Bernardi et al., 2004; Mekhail et al., 2005, 2007). Put together, these data suggest that protein dynamics is a common site of regulation mediated by stimuli-specific induction of ncRNAs.

Only recently has a role for ncRNAs gained a greater appreciation in the scientific community, growing beyond the housekeeping tasks of translation (rRNA, snoRNA, and tRNA) and splicing (U1, U2, etc.) to encompass numerous cellular pathways, including chromatin modification, transcriptional control, and posttranscriptional regulation (reviewed in Mattick, 2005; Nagano and Fraser, 2011). The lack of sequence conservation of these transcripts has been a fundamental drag on their acceptance as functional molecules. However, unlike protein-coding transcripts that require strict preservation of their open reading frames, ncRNA conservation relies on maintaining the integrity of their promoters, processing sites (Ponjavic et al., 2007), and secondary structures (Mayer et al., 2006, 2008; Ponjavic et al., 2007; Torarinsson et al., 2006). This is particularly applicable when comparing the mouse and human rDNA intergenic spacers because mRNA orthologs share an ~85% sequence identity (Makalowski and Boguski, 1998) and rRNA is ~92% identical, whereas there is only an ~40% sequence similarity in the IGS. Perhaps this lack of homology has lead to the delay in identifying ncRNAs expressed from this region because it has been perceived historically to be silent within the genome. The inducibility, presence of processing, and functionality of these stimuli-specific IGSRNA in nucleolar detention indicate the emerging importance of these transcripts.

In conclusion, we envision a system whereby extracellular cues trigger the expression of condition-specific ncRNAs transcribed from multiple IGS loci. The mature IGS transcripts capture NoDS-containing proteins and tether the molecular complexes to their sites of expression on the rDNA cassette. The possibility that a large number of proteins encode NoDS sequences suggests that nucleolar detention is most likely a more prevalent posttranslational regulatory mechanism than previously appreciated. This contribution provides the foundation for our understanding of the pathways involved in the

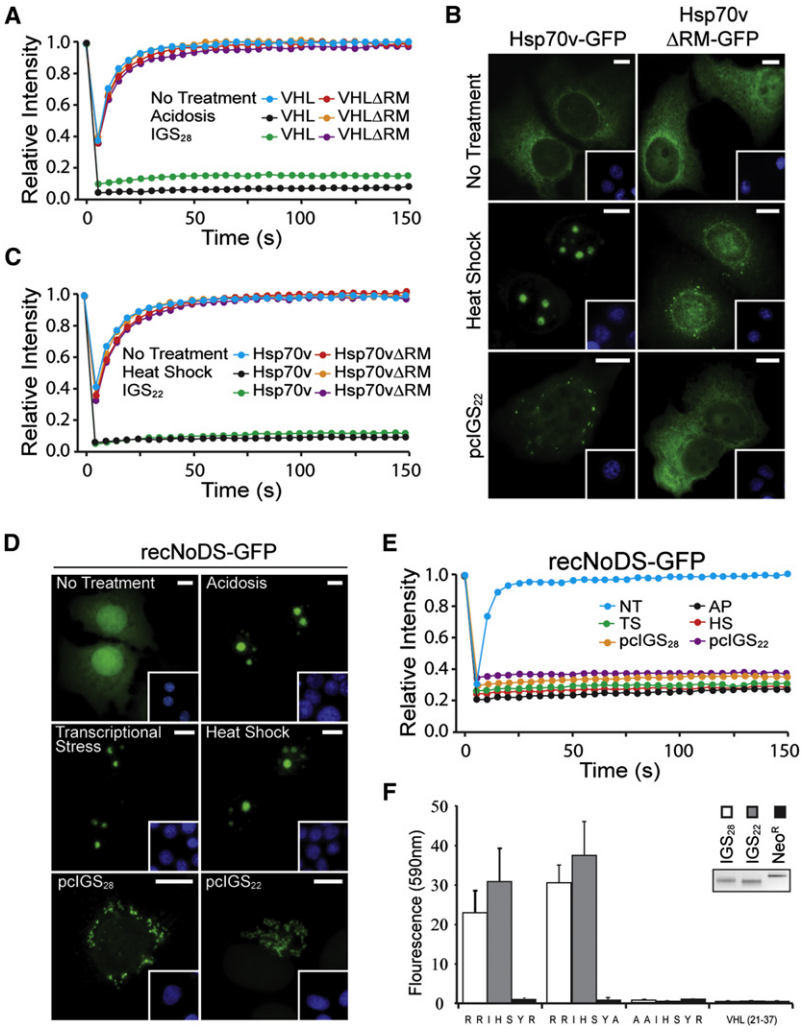

Figure 7. The NoDS Motif Is Required and Sufficient to Mediate Immobilization of Proteins by ncRNAs

(A) Quantification of FRAP data for VHL-GFP (VHL) or the arginine deletion mutant (VHLΔRM) in the presence of $pcIGS_{28}$ or during acidosis.

(B) The arginine motif is essential for the immobilization of Hsp70. Plasmids expressing Hsp70v-GFP or the $RR^{I}/_{L}$ motif deletion mutant Hsp70vΔRM-GFP were transfected into MCF-7 cells exposed to a heat shock treatment or co-transfected with $pcIGS_{22}$. Bars, 10 μm.

(C) Quantification of FRAP data for Hsp70v and Hsp70vΔRM.

(D) A reconstituted NoDS fused to GFP is sufficient to respond to extracellular cues and ectopic expression of IGSRNA. A plasmid encoding the amino acid sequence RRIHYSRLLVNQTELFV, fused to GFP and transfected into MCF-7 cells was exposed to acidosis, heat shock, transcriptional stress, IGS_{22}RNA and IGS_{28}RNA.

(E) Quantification of FRAP experiments for the recNoDS-GFP plasmid.

(F) IGS_{28}RNA and IGS_{22}RNA trigger precipitation of a recNoDS peptide. In vitro synthesized IGS_{28}RNA, IGS_{22}RNA and the Neo^{R} mRNA were produced (inset) and mixed with the recNoDS peptide and its mutants or the unrelated VHL (21–37) peptide and allowed to precipitate. Precipitated samples were analyzed for rhodamine fluorescence. Error bars represents the standard error of the mean from three independent repeats.

regulation of protein function by ncRNA-mediated nucleolar immobilization.

EXPERIMENTAL PROCEDURES

Details of the plasmids, primers, and antibodies can be found in Supplemental Information. Tissue culture, transfections, immunostaining, and western and northern blotting were carried out using standard procedures.

Stable Cell Lines and Treatments

Stable MCF-7 and HEK293 cells were produce with shRNA targeting the sequences 5′-GGCACTGTATTGCTACTGG (shRNA-22), 5′-TCTAGACAGG CGGGCCTTG (shRNA-28#1), 5′-TTAATTAATTCATTAATTCT (shRNA-28#2), and 5′-CGTCTTTTTCGAGAGTCTG (shPML). Acidification was done at 1% oxygen by either adding pH 6.0 media directly or by transferring cells to permissive media and naturally acidifying for 18–22 hr. Heat shock was performed by transferring cells to 42°C for 1 or 3 hr, then allowing cells to recover for up to 30 min at 37°C. Transcriptional stress was induced at 37°C through the addition of 4 μM ActiomycinD and 8 μM MG132 for 3 hr.

Photobleaching and Fluorescent In Situ Hybridization

Live cells were grown on 35 mm glass-bottom culture dishes and visualized by confocal microscopy (Zeiss LSM5 Pascal) in a 37°C and 5% CO_2 environmental chamber (Pecon). A 63× oil immersion lens with a 1.4 NA was controlled by Zeiss LSM5 Pascal software during bleaching and image acquisition on the AxioCam HRM camera. Bleached areas were exposed to three 100% power argon laser pulses at 488 nm, while imaging used 5% laser strength. FRAP experiments required images to be taken at 5 s intervals. Regions of interest were analyzed using ImageJ (National Institute of Health, Bethesda, MD) and quantification was described previously (Phair and Misteli, 2000). Briefly, relative intensity (I_r) of the bleached region was calculated as $I_r = (I_t/I_0)*(T_0/T_t)$, with I_t and I_0 being the mean intensity of the bleached region at time t or time zero (prior to photobleaching), respectively, while T_t and T_0 correspond to the total cellular intensity at the indicated times. FLIP analysis required the acquisition of images every 20 or 30 s immediately prior to three 100% laser pulses. Relative loss of cellular intensity was calculated as $I_r = (I_t/I_0)*(N_0/N_t)$, where I is the fluorescence intensity of the bleached cell and N is the intensity of a neighboring cell within the same field of vision. Results for each experiment were based on the mean relative intensity of at least 10 data sets normalized to background fluorescence. Pseudocolor gradients were applied to photo montages using Photoshop (Adobe), with red (high) and blue (low) intensity. Fluorescent in situ hybridization (FISH) of cells fixed in 4% paraformaldehyde for 10 min, followed by a 5 min incubation in methanol, was performed with 5′ and 3′ digoxigenin-labeled oligonucleotide IGS_{28}RNA anti-sense or IGS_{28}RNA sense probes in a 50% formamide/DIG hybridization (Roche) solution at 37°C. Following hybridization, cells were washed in 0.2% SSC and probes were detected with an α-digoxigenin (Roche) antibody. Counterstaining of DNA for immunofluorescence or RNA-FISH was performed with Hoectsh 33342.

Chromatin and RNA Immunoprecipitation

Chromatin immunoprecipitation was carried out according manufacturers protocol using the EZ ChIP™ kit (Upstate Biotechnologies). RNA immunoprecipitation was carried out on MCF-7 cells growth in acidosis permissive media. Cells were harvested in lysis buffer (100 mM NaCL, 0.5% Igepal, 20 mM Tris [pH7.6], 5 mM $MgCl_2$, and 1 mM Na_3VO_4) and sonicated prior to incubation

with FLAG-beads (Sigma). Following washes, RNA was extracted from samples and 2% inputs for RT-PCR.

RNA Extraction and Analysis

Total RNA was isolated from MCF-7, HEK293 and WI-38 cells with Trizol reagent (Invitrogen), followed by treatment with DNaseI for 2 hr and phenol/chloroform and ethanol precipitation. RNA was quantified and cDNA synthesis was carried out using the High Capacity cDNA Synthesis Kit (Applied Bioscience). Semiquantitative PCR analyses were performed using primers specific to the IGS_{16}RNA (5′-CTCGAACTCCCGACCTAGTG and 5′- AGCAAACGATG AACGTGACA) IGS_{22}RNA (5′- AACACCACCTCCTTGACCTG and 5′- ACAGAG AGAAGGCCCTAGCC) IGS_{28}RNA (5′-CCTTCCACGAGAGTGAGAAG and 5′-CCTCCAGAAGGGAGAGAGAGA) with β-actin used as a control. Northern blotting used IGSRNA probes corresponding to the GeneBank human rDNA sequences (U13369): IGS_{28} (nt: 27395-27793) and IGS_{22} (nt:20998-22082).

Cell Fractionation

Cell fractionation was previously described (Andersen et al., 2002). RNA purification was subsequently performed on fractionated samples using Trizol.

GST Pulldown Assay

Commercially available GST and GST-Hsp70 (3 μg) (USBiologicals) were incubated for 2 hr with 100 ng of IGS_{28}RNA, IGS_{22}(g)RNA, IGS_{22}RNA or neomycin resistance mRNA (Neo^R) transcribed in vitro using the MAXIscript kit (Ambion) prior to the addition of GST beads (GE Healthcare). Following six washes with 20 mM HEPES (pH7.9), 150 mM NaCl, 0.5 mM EDTA, 10% Glycerol, 0.1% Triton X-100, 0.1% RNase Inhibitor, and 1 mM DTT, RNA was extracted with Trizol reagent and cDNA was synthesis. PCR was performed to detect IGS_{28}, IGS_{22}(g), IGS_{22} and Neo^R.

Peptides and Peptide Precipitation Assay

Peptides were synthesized by W.M. Keck Foundation Biotechnology Resource Laboratory (New Haven, CT) and fused to a fluorescent Rhodamine (Rho) dye at the amino-terminus. Precipitation of the peptides was performed by mixing equal amounts of peptides with 2 μg of total cellular RNA as a carrier and 80 ng of IGS_{28}RNA, IGS_{22}RNA or neomycin resistance mRNA transcribed in vitro. Following a 1 hr incubation at 4°C samples were spun at 15,000 rpm for 15 min. Supernatants were removed and pellets were resuspended in 0.1% SDS and transferred to a 96-well plate for analysis of rhodamine fluorescence by the SpectraMax M2 (Molecular Devices). Data represent a minimum of three independent repeats.

ACCESSION NUMBERS

Sequences of the IGSRNA have been deposited into GenBank under the accession numbers: IGS_{28}RNA (JN872552 to JN872556) and IGS_{22}RNA (JN872557 to JN872559).

SUPPLEMENTAL INFORMATION

Supplemental Information includes Supplemental Experimental Procedures, seven figures, and two movies and can be found with this article online at doi:10.1016/j.molcel.2011.12.012.

ACKNOWLEDGMENTS

We thank Jocelyn Côté and Laura Trinkle-Mulcahy for critical reading of the manuscript and Josianne Payette for her technical expertise. This work was supported by grants from the Canadian Institute of Health Research (CIHR) to S.L.

Received: March 29, 2011
Revised: August 11, 2011
Accepted: October 27, 2011
Published: January 26, 2012

REFERENCES

Andersen, J.S., Lyon, C.E., Fox, A.H., Leung, A.K., Lam, Y.W., Steen, H., Mann, M., and Lamond, A.I. (2002). Directed proteomic analysis of the human nucleolus. Curr. Biol. *12*, 1–11.

Andersen, J.S., Lam, Y.W., Leung, A.K., Ong, S.E., Lyon, C.E., Lamond, A.I., and Mann, M. (2005). Nucleolar proteome dynamics. Nature *433*, 77–83.

Anderson, P., and Kedersha, N. (2009). RNA granules: post-transcriptional and epigenetic modulators of gene expression. Nature reviews *10*, 430–436.

Bernardi, R., Scaglioni, P.P., Bergmann, S., Horn, H.F., Vousden, K.H., and Pandolfi, P.P. (2004). PML regulates p53 stability by sequestering Mdm2 to the nucleolus. Nat. Cell Biol. *6*, 665–672.

Boulon, S., Westman, B.J., Hutten, S., Boisvert, F.M., and Lamond, A.I. (2010). The nucleolus under stress. Mol. Cell *40*, 216–227.

Buchan, J.R., and Parker, R. (2009). Eukaryotic stress granules: the ins and outs of translation. Mol. Cell *36*, 932–941.

Chen, D., and Huang, S. (2001). Nucleolar components involved in ribosome biogenesis cycle between the nucleolus and nucleoplasm in interphase cells. J. Cell Biol. *153*, 169–176.

Clemson, C.M., Hutchinson, J.N., Sara, S.A., Ensminger, A.W., Fox, A.H., Chess, A., and Lawrence, J.B. (2009). An architectural role for a nuclear noncoding RNA: NEAT1 RNA is essential for the structure of paraspeckles. Mol. Cell *33*, 717–726.

Dundr, M., Hoffmann-Rohrer, U., Hu, Q., Grummt, I., Rothblum, L.I., Phair, R.D., and Misteli, T. (2002). A kinetic framework for a mammalian RNA polymerase in vivo. Science *298*, 1623–1626.

Emmott, E., and Hiscox, J.A. (2009). Nucleolar targeting: the hub of the matter. EMBO Rep. *10*, 231–238.

Fox, A.H., and Lamond, A.I. (2010). Paraspeckles. Cold Spring Harb. Perspect. Biol. *2*, 1–14.

Hager, G.L., McNally, J.G., and Misteli, T. (2009). Transcription dynamics. Mol. Cell *35*, 741–753.

Hillis, D.M., and Dixon, M.T. (1991). Ribosomal DNA: molecular evolution and phylogenetic inference. Q. Rev. Biol. *66*, 411–453.

Honda, R., Tanaka, H., and Yasuda, H. (1997). Oncoprotein MDM2 is a ubiquitin ligase E3 for tumor suppressor p53. FEBS Lett. *420*, 25–27.

Houtsmuller, A.B., Rademakers, S., Nigg, A.L., Hoogstraten, D., Hoeijmakers, J.H., and Vermeulen, W. (1999). Science. Action of DNA repair endonuclease ERCC1/XPF in living cells *284*, 958–961.

Jacobson, M.R., Cao, L.G., Wang, Y.L., and Pederson, T. (1995). Dynamic localization of RNase MRP RNA in the nucleolus observed by fluorescent RNA cytochemistry in living cells. J. Cell Biol. *131*, 1649–1658.

Jolly, C., and Lakhotia, S.C. (2006). Human sat III and Drosophila hsr omega transcripts: a common paradigm for regulation of nuclear RNA processing in stressed cells. Nucleic Acids Res. *34*, 5508–5514.

Jolly, C., Usson, Y., and Morimoto, R.I. (1999). Rapid and reversible relocalization of heat shock factor 1 within seconds to nuclear stress granules. Proc. Natl. Acad. Sci. USA *96*, 6769–6774.

Jolly, C., Metz, A., Govin, J., Vigneron, M., Turner, B.M., Khochbin, S., and Vourc'h, C. (2004). Stress-induced transcription of satellite III repeats. J. Cell Biol. *164*, 25–33.

Kaiser, T.E., Intine, R.V., and Dundr, M. (2008). De novo formation of a subnuclear body. Science *322*, 1713–1717.

Kedersha, N., Cho, M.R., Li, W., Yacono, P.W., Chen, S., Gilks, N., Golan, D.E., and Anderson, P. (2000). Dynamic shuttling of TIA-1 accompanies the recruitment of mRNA to mammalian stress granules. J. Cell Biol. *151*, 1257–1268.

Kruhlak, M.J., Lever, M.A., Fischle, W., Verdin, E., Bazett-Jones, D.P., and Hendzel, M.J. (2000). Reduced mobility of the alternate splicing factor (ASF) through the nucleoplasm and steady state speckle compartments. J. Cell Biol. *150*, 41–51.

Lakhotia, S.C. (1989). The 93D heat shock locus of Drosophila melanogaster: modulation by genetic and developmental factors. Genome *31*, 677–683.

Lohrum, M.A., Ludwig, R.L., Kubbutat, M.H., Hanlon, M., and Vousden, K.H. (2003). Regulation of HDM2 activity by the ribosomal protein L11. Cancer Cell *3*, 577–587.

Makalowski, W., and Boguski, M.S. (1998). Evolutionary parameters of the transcribed mammalian genome: an analysis of 2,820 orthologous rodent and human sequences. Proc. Natl. Acad. Sci. USA *95*, 9407–9412.

Mao, Y.S., Sunwoo, H., Zhang, B., and Spector, D.L. (2011). Direct visualization of the co-transcriptional assembly of a nuclear body by noncoding RNAs. Nat. Cell Biol. *13*, 95–101.

Matera, A.G., Izaguire-Sierra, M., Praveen, K., and Rajendra, T.K. (2009). Nuclear bodies: random aggregates of sticky proteins or crucibles of macromolecular assembly? Dev. Cell *17*, 639–647.

Mattick, J.S. (2005). The functional genomics of noncoding RNA. Science *309*, 1527–1528.

Maxwell, P.H., Wiesener, M.S., Chang, G.W., Clifford, S.C., Vaux, E.C., Cockman, M.E., Wykoff, C.C., Pugh, C.W., Maher, E.R., and Ratcliffe, P.J. (1999). The tumour suppressor protein VHL targets hypoxia-inducible factors for oxygen-dependent proteolysis. Nature *399*, 271–275.

Mayer, C., Schmitz, K.M., Li, J., Grummt, I., and Santoro, R. (2006). Intergenic transcripts regulate the epigenetic state of rRNA genes. Mol. Cell *22*, 351–361.

Mayer, C., Neubert, M., and Grummt, I. (2008). The structure of NoRC-associated RNA is crucial for targeting the chromatin remodelling complex NoRC to the nucleolus. EMBO Rep. *9*, 774–780.

McStay, B., and Grummt, I. (2008). The epigenetics of rRNA genes: from molecular to chromosome biology. Annu. Rev. Cell Dev. Biol. *24*, 131–157.

Mekhail, K., Gunaratnam, L., Bonicalzi, M.E., and Lee, S. (2004). HIF activation by pH-dependent nucleolar sequestration of VHL. Nat. Cell Biol. *6*, 642–647.

Mekhail, K., Khacho, M., Carrigan, A., Hache, R.R., Gunaratnam, L., and Lee, S. (2005). Regulation of ubiquitin ligase dynamics by the nucleolus. J. Cell Biol. *170*, 733–744.

Mekhail, K., Rivero-Lopez, L., Al-Masri, A., Brandon, C., Khacho, M., and Lee, S. (2007). Identification of a common subnuclear localization signal. Mol. Biol. Cell *18*, 3966–3977.

Milarski, K.L., and Morimoto, R.I. (1989). Mutational analysis of the human HSP70 protein: distinct domains for nucleolar localization and adenosine triphosphate binding. J. Cell Biol. *109*, 1947–1962.

Misteli, T. (2001a). The concept of self-organization in cellular architecture. J. Cell Biol. *155*, 181–185.

Misteli, T. (2001b). Protein dynamics: implications for nuclear architecture and gene expression. Science *291*, 843–847.

Nagano, T., and Fraser, P. (2011). No-nonsense functions for long noncoding RNAs. Cell *145*, 178–181.

Phair, R.D., and Misteli, T. (2000). High mobility of proteins in the mammalian cell nucleus. Nature *404*, 604–609.

Ponjavic, J., Ponting, C.P., and Lunter, G. (2007). Functionality or transcriptional noise? Evidence for selection within long noncoding RNAs. Genome Res. *17*, 556–565.

Rizzi, N., Denegri, M., Chiodi, I., Corioni, M., Valgardsdottir, R., Cobianchi, F., Riva, S., and Biamonti, G. (2004). Transcriptional activation of a constitutive heterochromatic domain of the human genome in response to heat shock. Mol. Biol. Cell *15*, 543–551.

Rubbi, C.P., and Milner, J. (2003). Disruption of the nucleolus mediates stabilization of p53 in response to DNA damage and other stresses. EMBO J. *22*, 6068–6077.

Sasaki, Y.T., Ideue, T., Sano, M., Mituyama, T., and Hirose, T. (2009). MENepsilon/beta noncoding RNAs are essential for structural integrity of nuclear paraspeckles. Proc. Natl. Acad. Sci. USA *106*, 2525–2530.

Scherl, A., Couté, Y., Déon, C., Callé, A., Kindbeiter, K., Sanchez, J.C., Greco, A., Hochstrasser, D., and Diaz, J.J. (2002). Functional proteomic analysis of human nucleolus. Mol. Biol. Cell *13*, 4100–4109.

Shaw, P.J., and Jordan, E.G. (1995). The nucleolus. Annu. Rev. Cell Dev. Biol. *11*, 93–121.

Shou, W., Seol, J.H., Shevchenko, A., Baskerville, C., Moazed, D., Chen, Z.W., Jang, J., Shevchenko, A., Charbonneau, H., and Deshaies, R.J. (1999). Exit from mitosis is triggered by Tem1-dependent release of the protein phosphatase Cdc14 from nucleolar RENT complex. Cell *97*, 233–244.

Stark, L.A., and Dunlop, M.G. (2005). Nucleolar sequestration of RelA (p65) regulates NF-kappaB-driven transcription and apoptosis. Mol. Cell. Biol. *25*, 5985–6004.

Torarinsson, E., Sawera, M., Havgaard, J.H., Fredholm, M., and Gorodkin, J. (2006). Thousands of corresponding human and mouse genomic regions unalignable in primary sequence contain common RNA structure. Genome Res. *16*, 885–889.

Tschochner, H., and Hurt, E. (2003). Pre-ribosomes on the road from the nucleolus to the cytoplasm. Trends Cell Biol. *13*, 255–263.

Weber, J.D., Taylor, L.J., Roussel, M.F., Sherr, C.J., and Bar-Sagi, D. (1999). Nucleolar Arf sequesters Mdm2 and activates p53. Nat. Cell Biol. *1*, 20–26.

Welch, W.J., and Feramisco, J.R. (1984). Nuclear and nucleolar localization of the 72,000-dalton heat shock protein in heat-shocked mammalian cells. J. Biol. Chem. *259*, 4501–4513.